ELSEVIER

Biophysical Chemistry 72 (1998) 73–85

Biophysical Chemistry

Self-organizing molecular networks

P. Stange[a], D. Zanette[a,1], A. Mikhailov[a], B. Hess[b,*]

[a]*Abteilung Physikalische Chemie, Fritz-Haber-Institut der Max-Planck-Gesellschaft, Faradayweg 4-6, D-14195 Berlin, Germany*
[b]*Max-Planck-Institut für medizinische Forschung, Jahnstrasse 29, D-69120 Heidelberg, Germany*

Revision received 8 January 1998; accepted 13 January 1998

Abstract

Strong diffusional mixing and short delivery times typical for micrometer and sub-micrometer reaction volumes lead to a special situation where the turnover times of individual enzyme molecules become the largest characteristic time scale of the chemical kinetics. Under these conditions, populations of cross-regulating allosteric enzymes form molecular networks that exhibit various kinds of self-organized coherent collective dynamics.

Keywords: Enzymic reactions; Allosteric regulation; Diffusion; Synchronization; Microvolumes

1. Introduction

A living cell is a tiny chemical reactor where tens of thousands of chemical reactions can simultaneously go on. The very fact that these reactions proceed in a regular and predictable manner, despite thermal fluctuations and variations in environmental conditions, already indicates a high degree of organization in this system. The biochemical activity of a cell can be compared with operation of a large industrial factory where certain parts are produced by a system of machines. Products of one machine are then used by other machines for manufacturing of their products or for regulation of their functions.

Two possible modes of operation of such a factory can be imagined. In the asynchronous mode, the parts produced by all machines are first deposited and accumulated in a common store. They are taken back from this store by other machines, when the parts are needed for further production. This kind of organization is not however optimal, since it requires large storage facilities and many transactions. It becomes deficient when intermediate products are potentially unstable and can easily be lost or damaged during the storage process.

When the synchronous operation mode is employed, the intermediate products, required for a certain operation step in a given machine, are released by other machines and become available exactly at the moment when they are needed. Hence, large storage facilities are eliminated and the entire process may run much faster.

For a living cell, the role of the ‘machines’ is played by individual enzyme molecules. The ‘parts’ are intermediate product molecules, which may also serve to allosterically regulate the catalytic activity of other enzymes. Some time ago, we have suggested that under certain conditions the biochemical subsystems

* Corresponding author.

[1] Permanent address: Consejo Nacional de Investigaciones Cientificas y Tecnicas, Centro Atomico Bariloche and Instituto Balseiro, 8400 Bariloche, Argentina.

0301-4622/98/$19.00
PII S0301-4622(98)00124-0

of a cell may operate in the synchronous mode [1–5]. When this occurs, the entire population of reacting and interacting molecules can be viewed as a highly connected dynamic molecular network.

The synchronous manufacturing process implies much more complicated management than the asynchronous operation mode. In a real factory, this is achieved by careful planning and detailed external control of the production. Such a rigid external control at a molecular level inside a cell is however impossible. The coherence, underlying the synchronous production, emerges in this case as a natural consequence of interactions between individual elements, i.e. it represents a special kind of self-organization phenomena. Remarkably, the predictable coherent operation of the complex molecular machinery must be maintained under very stringent conditions, when strong thermal fluctuations are present and the parts needed in the assembly lines of the cell are often transported just by random Brownian motion of molecules.

If the asynchronous mode is employed, functioning of an industrial factory is well described by a scheme indicating involved machines, intermediate products, and performed operations. If, furthermore, the operation rates of the machines and the rate of supply of the initial raw materials are known, the efficiency of the factory, i.e. its overall production rate, can easily be estimated.

In contrast to this, fine dynamical coordination of different operations in the synchronous mode requires much more detailed information about properties of individual machines and their operation cycles. Such system parameters as the time needed for transportation and delivery of intermediate products and the duration of a single machine cycle become significant. Moreover, the mechanistic details of individual machine cycles, such as, for example, the moment inside a cycle when the product is released and the duration of the subsequent recovery phase of the machine leading to full restoration of its operation capacity, are already important.

For a biochemical system, the asynchronous operation mode corresponds to the classical kinetic regime. This regime can indeed be completely characterized by its reaction scheme and by the information about rate constants of elementary reaction steps. The above arguments show, however, that the knowledge of the reaction scheme and of the rate constants would not be sufficient to describe non-classical synchronous kinetics. When this different regime is realized, properties of molecular turnover cycles in individual enzyme molecules become equally essential in determining the system performance.

The self-organization processes, leading to emergence of coherent molecular networks, are different from the self-organization phenomena in classical reaction-diffusion systems. The latter typically lead to the appearance of complex spatiotemporal patterns [6] or to the development of slow kinetic oscillations [7,8]. They are not, however, characterized by the presence of rigid microscopic correlations between individual molecular reaction events which represent a distinctive feature of a molecular network.

Indeed, slow oscillations may also develop in the considered above factory operating in the asynchronous regime. They would then mean that, as a result of a dynamic instability, the amounts of various intermediate parts in the store are slowly changing with time, on the characteristic temporal scales which are much longer than the duration of operation cycles of individual involved machines. The appearance of such oscillations does not, of course, influence the principal functional organization of the production process and does not lead to rigid correlations between individual machine cycles.

Emergence and functioning of molecular networks refers, therefore, to a different form of self-organization which is expressed at a level of correlations and synchrony in terms of individual molecular dynamics of a reacting population of molecules.

In the next section we formulate the conditions under which a population of allosteric enzyme molecules may constitute a molecular network. An example of a simple enzymatic reaction exhibiting a transition to the microscopically coherent kinetic regime is considered in Section 3. More general questions of synchronization in systems formed by interacting networks are analyzed in Section 4. The last section contains a discussion of obtained results and of their significance for molecular biology of a cell.

2. Emergence of molecular networks

The conditions for microscopic self-organization of chemical reactions in small spatial volumes are deter-

mined by relations between principal time scales of the involved physical and chemical processes. Estimates of these time scales can be obtained by considering a biochemical system formed by enzyme molecules whose activity is allosterically regulated by intermediate product molecules of a smaller molecular weight.

We assume that the reaction proceeds in a small compartment representing a single globular volume filled with liquid. The molecules inside the compartment perform random diffusive motion described by the Fick law.

The mixing time, t_{mix}, is defined as the time after which a regulatory molecule, released at some point in the volume, can be found with equal probability anywhere inside it. If the volume has the linear size L and the diffusion constant of the regulatory molecules is D, the mixing time can be estimated, in the order of magnitude, as

$$t_{mix} = L^2 / D \quad (1)$$

Another important characteristic time of the process is the traffic time, $t_{traffic}$, which is defined as follows: suppose that we have released a regulatory particle somewhere inside the volume that contains only one target enzyme molecule. Then $t_{traffic}$ represents the characteristic time after which the regulatory particle will find this enzyme molecule and bind itself to the atomic target group on its surface.

It should be noted that the last stage of this process could actually be quite complicated and involve docking by electrostatic interactions and two-dimensional diffusion of the regulatory molecule over the surface of the enzyme until the target site is reached [9,10]. In our simple treatment we neglect all these possible complications and assume that the regulatory molecule performs free Brownian motion in the volume until it touches a small target of radius R attached to the surface of the enzyme molecule. Once touching has occurred, the regulatory molecule becomes bound to the target site.

Because the molecular weight of enzymes is larger than that of the regulatory molecules, the targets can be viewed as immobile. Under these conditions, the characteristic traffic time can be estimated using the concepts of the theory of diffusion-controlled reactions [11,12]. In the order of magnitude, it is given by (cf. [3,13,14]):

$$t_{traffic} = \frac{L^3}{DR} \quad (2)$$

where R is the radius of a target (if the size of the atomic target group in the enzyme is comparable to the size of a regulatory molecule, it should be replaced by the sum of the two respective radii). The traffic time is related to the mixing time as $t_{traffic} \sim (L/R)t_{mix}$.

To obtain numerical estimates of mixing and traffic times, we take $R = 1–10$ nm as the characteristic size of the atomic target group and $D = 10^{-5}–10^{-6}$ cm^2/s as the diffusion constant of the regulatory molecules. For a compartment of size $L = 1$ μm this yields the mixing time $t_{mix} = 1–10$ ms and the traffic time $t_{traffic} = 0.1–10$ s. For smaller compartments of size $L = 0.1$ μm the estimates are $t_{mix} = 0.01–0.1$ ms and $t_{traffic} = 0.1–10$ ms. We see that the traffic time depends strongly on the compartment size (as the cube of L). This high sensitivity on the volume size already indicates that one should expect very special kinetic regimes inside small cells and cellular compartments.

The traffic time shows the time needed for a regulatory molecule to find a given molecular target. If the volume contains N such targets and they are independently and randomly distributed inside it, the transit time needed by a regulatory molecule to find one of the targets can be estimated as $t_{transit} = (1/N)t_{traffic}$ or explicitly as:

$$t_{transit} = \frac{L^3}{NDR} \quad (3)$$

Note that $L_{corr} = (Dt_{transit})^{1/2}$ yields the mean distance passed by the regulatory molecule before it finds a target and this characteristic length can be considered as the correlation radius of the reaction. This distance can be compared with the linear size L of the reaction volume.

When $L \gg L_{corr}$, the target will be found in a close proximity of the point where the regulatory product molecule has been released. Since the regulatory molecules, conveying information about the reaction events, are trapped in this case not far from the points where they have been produced, they cannot maintain long-range correlations in the reacting system.

A completely different situation is found if the condition $L < L_{corr}$ is satisfied. Now, the first target is found by the regulatory molecule only after it has

traveled extensively through the reaction volume and has crossed it many times. It means that the regulatory molecule would be able, with equal probability, to find any of N enzymes in the population, no matter where they are located inside the volume.

The latter condition can also be expressed in terms of the characteristic times of the diffusion problem, i.e. can be written as:

$$t_{\mathrm{mix}} \ll t_{\mathrm{transit}} \tag{4}$$

When the transit time is much larger than the mixing time, the first target is found with equal probability anywhere in the volume.

According to Eq. (3), the transit time is inversely proportional to the total number N of enzyme molecules. Therefore, the condition (Eq. (4)) can be satisfied only for sufficiently small numbers of the enzymes. By putting $t_{\mathrm{mix}} = t_{\mathrm{transit}}$, we derive the estimate for the critical number of the enzyme molecules:

$$N_{\mathrm{cr}} = \frac{L}{R} \tag{5}$$

Thus, it is controlled in the order of magnitude only by two parameters: the linear size L of the reaction volume and the radius R of the atomic target group on the surface of the enzyme molecule. When the number N of enzyme molecules is less than N_{cr}, the product-mediated allosteric interactions between enzymes extend over the entire reaction volume. Note that Eq. (5) yields the critical enzyme concentration

$$c_{\mathrm{cr}} = \frac{1}{L^2 R} \tag{6}$$

which decreases with the linear size L of the volume.

Taking $R = 1–10$ nm as the characteristic size of an enzyme target group, we see that the critical number of enzyme molecules in the volume of size $L = 1$ μm is $N_{\mathrm{cr}} = 100–1000$, which corresponds to the enzymic concentrations of $c_{\mathrm{cr}} = 10^{-7}–10^{-6}$ M. For a smaller compartment of size $L = 0.1$ μm we obtain $N_{\mathrm{cr}} = 10–100$ and $c_{\mathrm{cr}} = 10^{-5}–10^{-4}$ M.

The above characteristic diffusion times can be compared with the duration τ_0 of a single catalytic molecular cycle. This time has not been directly measured but some estimates of its magnitude could be obtained by measuring the maximal turnover rate of an enzymic reaction. It is believed that this rate, reached under the condition of the substrate saturation, is controlled only by the molecular turnover [10]. Hence, τ_0 can be roughly estimated as the inverse of the maximal turnover rate. Thus derived, the estimates for τ_0 may range, depending on a particular enzyme, from as small as fractions of a microsecond to several seconds [15]. If we consider relatively slow enzymes, the typical values would lie in the interval $\tau_0 = 10–100$ ms.

These characteristic microscopic molecular times can be compared with the characteristic diffusion times of the reaction. For the reactions in micrometer and submicrometer volumes involving hundreds or thousands of enzyme molecules this time may be much larger than both the mixing and the transit times in the reaction volume,

$$\tau_0 \gg t_{\mathrm{transit}} \gg t_{\mathrm{mix}} \tag{7}$$

This is a remarkable result. In a macroscopic system, all characteristic kinetic times of a chemical reaction are usually much longer than the duration of a single molecular reaction event and therefore these events can be treated as instantaneous. This forms the basis of the traditional kinetic theory formulated in terms of the Markov random processes. We see, however, that in very small spatial volumes for enzymic chemical reactions the opposite limit may be realized, so that the characteristic times of internal molecular dynamics of the enzymes become larger than the kinetic times of the reaction. When this occurs, the theoretical description of a chemical reaction should be essentially modified.

The considered system can be viewed as a population of active macromolecules that operate like molecular machines [16]. Each internal molecular cycle of an enzyme results in the conversion of a substrate molecule into a molecule of the product. The cycle represents a sequence of conformation changes that can be understood as continuous motion along an internal reaction coordinate. For allosteric enzymes, the molecular cycles can be externally controlled by binding of regulatory molecules. Generally, arrival of a regulatory molecule can lead either to acceleration or slowing down at some stages of a molecular cycle.

When regulatory molecules are produced by enzymes in the same population, this leads to interactions (or communication) between the cycles of different enzyme molecules. If Eq. (7) holds, the characteristic transport times of regulatory molecules

between the enzymes are short as compared with the molecular cycle duration. Furthermore, if the transit time is larger than the mixing time in the volume, a regulatory molecule released by a given enzyme can influence, with equal probability, the catalytic cycle of any other enzyme in the population. We have earlier suggested [5] that such interacting populations of active macromolecules should be called 'molecular networks'.

In the presence of strong allosteric interactions, the internal dynamics of individual enzyme molecules in such a network can be so significantly influenced by the dynamics of other enzymes that the whole system would perform coherent collective evolution in the multidimensional phase space of internal reaction coordinates, i.e. behave as a single dynamical object. This coherence would be manifested in rigid correlations between the individual catalytic cycles and the moments when the product molecules are released by different enzymes.

3. Coherent molecular dynamics

To show the possibility of a transition to coherent collective behavior of an enzymic population, we consider the reaction

$$S + E \rightarrow ES \rightarrow E + P, \; P \rightarrow 0 \tag{8}$$

where binding of substrate S by enzyme E is allosterically activated by product P. If the substrate concentration is kept constant, this reaction does not exhibit macroscopic rate oscillations [7]. However, in small spatial volumes for sufficiently high intensities of the allosteric regulation periodic spiking of the catalytic activity of the whole enzymic population can develop. This spiking is a result of the synchronization of individual molecular cycles and thus represents an effect of coherent collective molecular dynamics.

The molecular mechanism of the reaction (Eq. (8)) includes several stages. An enzyme molecule E binds a molecule S of the substrate and the substrate-enzyme complex ES begins a sequence of conformational changes that ends, after time τ_1, in the release of the product molecule P. When the product molecule has left, the conformation of the enzyme molecule returns to the initial state. This recovery stage takes time τ_2 during which binding of a substrate molecule cannot occur. Hence, only after the time $\tau_0 = \tau_1 + \tau_2$, which represents the duration of a molecular catalytic cycle, the enzyme molecule can begin a new cycle. Note that thus the molecular cycle has much in common with the sequence of transitions in an excitable neuron [17].

Fig. 1 schematically shows an individual enzymatic molecular cycle. The small black circle represents the enzyme in the initial ground state, the red circle indicates the enzyme that has bound a substrate molecule and goes through a sequence of changes that would lead to the release of the product molecule. The enzyme releasing the product molecule is represented by a white circle. The enzyme going through the subsequent recovery stage is shown as a blue circle.

The initial binding of a substrate molecule is allosterically regulated. We assume that the probability of binding of a substrate by an enzyme in its resting conformation is small. It becomes however greatly increased if an additional regulatory molecule is bound to a different site on the surface of the enzyme and this, by means of cooperative interactions within the enzyme macromolecule, facilitates the binding of the substrate. It is assumed that the enzyme has only one binding site for a regulatory molecule and its binding can only take place when an enzyme is in its resting state, i.e. when the previous catalytic cycle is finished. The regulatory molecule departs from the enzyme when the catalytic cycle begins.

In the considered hypothetical reaction (8), the regulatory role is played by the product molecules and thus the reaction is effectively autocatalytic. The product molecules decay and therefore their lifetimes are finite. To exclude immediate triggering of a new molecular catalytic cycle by the product molecule that has just been released by the enzyme, we assume that the lifetime of a product molecule is shorter than the molecular recovery time τ_2. Under this condition, the product molecules can usually execute their regulatory roles only by traveling through the volume and initiating the catalytic cycles of other enzymes in the population. If γ is the decay rate of product molecules, this condition can be expressed as $\gamma\tau_2 > 1$.

Because of thermal molecular fluctuations, the cycle duration would have a certain statistical dispersion. Apparently, the relative magnitude of this dis-

persion may strongly depend on the reaction conditions and the particular kind of enzymes. In our analysis, we consider a situation when this statistical dispersion is weak, i.e. the statistical variations of the period τ_0 are small as compared with its mean value. Under this assumption, the cycle can be approximately described as deterministic motion along a certain internal 'reaction coordinate'. The motion begins after binding a substrate molecule and ends when, after releasing the product, the enzyme returns to its original state. This cycle has a fixed duration τ_0.

It is convenient to introduce the phase variable ϕ which would characterize motion along the cyclic reaction coordinate. This variable is defined as the relative time needed to reach a given molecular state by moving along the reaction path. In the initial substrate-free state $\phi = 0$. The product molecule is released at the state with the phase $\phi = \tau_1/\tau_0$. The cycle ends when the phase reaches the value $\phi = (\tau_1 + \tau_2)/\tau_0 = 1$.

Using this concept, the dynamics of a single enzyme molecule can be described as operation of an automaton, similar to that used by Wiener and Rosenblueth in their modeling of individual neurons [17] (see also [18]). We have constructed the automaton model of the considered reaction in our previous publications [4,5].

The model includes the parameters α_0 and α_1 that characterize binding rates of a substrate molecule by a single molecule of the enzyme. The parameter α_0 determines the probability per unit time of spontaneous non-activated binding of a substrate molecule. The parameter α_1 represents the probability that, if the compartment contains a single regulatory product molecule, this molecule would lead per unit time to an activated binding of the substrate molecule by a given enzyme molecule.

For convenience, the time is divided in this model into small discrete steps Δt. The probabilities per a single time step of non-activated and activated substrate binding events are therefore been given by $w_0 = \alpha_0\Delta t$ and $w_1 = \alpha_1\Delta t$. The decay probability of a product molecule per a single time step is $g = \gamma\Delta t$.

In the discrete approximation, an individual cycle consists of $K = \tau_0/\Delta t$ and the product molecules are released after $K_1 = \tau_1/\Delta t$ time steps from the cycle initiation. Each automaton corresponds to a single enzyme and has K internal states described by the integer phase variable Φ. The state of the automaton i at the next discrete time moment T is determined by the algorithm [4,5]:

$$\Phi_i(T+1) = \begin{cases} \Phi_i(T)+1, \text{ if } 0 < \Phi_i(T) < K \\ 0, \text{ if } \Phi_i(T) = K \\ 1, \text{ with probability } w(m), \text{ if } \Phi_i(T) = 0 \\ 0, \text{ with probability } 1-w(m), \text{ if } \Phi_i(T) = 0 \end{cases} \quad (9)$$

The probability w of cycle initiation depends on the number m of product molecules in the reaction volume:

$$w(m) = 1-(1-w_0)(1-w_1)^m \quad (10)$$

The products decay with the probability g per time step. The probability $\pi(m,m')$ that m' out of m product molecules decay within a single time step is therefore given by the binomial distribution:

$$\pi(m',m) = \frac{m!}{m'!(m-m')!} g^{m'}(1-g)^{m-m'} \quad (11)$$

Taking into account both production and decay processes, the number of product molecules in the reaction volume at the next time step is

$$m(T+1) = m(T) + \sum_{i=1}^{N} \delta(\Phi_i(T) - K_1) - m' \quad (12)$$

where N is the total number of enzymes. The number m' of disappearing product molecules is random; it obeys the probability distribution (Eq. (11)) where $m = m(T)$.

Below we present the typical results which are obtained using this model under different assumptions about the intensity of allosteric regulation which is specified by the parameter α_1. As the initial condition in our simulations, we have always chosen a state with random distributions over the cycle phases and a small number of the product molecules. The population consists of $N = 400$ enzyme molecules.

Fig. 2 illustrates the kinetic regime of the reaction in Eq. (1) when the intensity of allosteric regulation is low and therefore the individual molecular cycles are not correlated. The upper part of Fig. 2a displays the individual activity of 14 enzymes which have been at random selected among the entire population. The

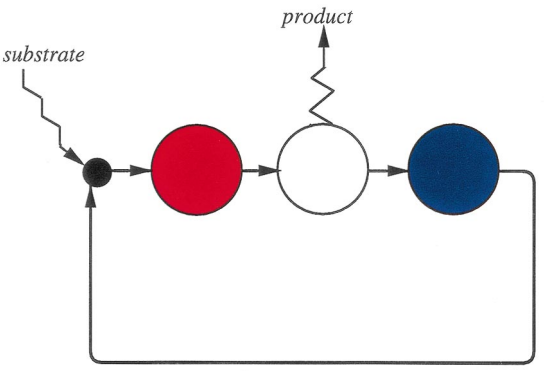

Fig. 1. Schematic representation of a single molecular turnover cycle. The black dot indicates the enzyme molecule in the initial free state. The red circle indicates a sequence of states corresponding to the substrate-enzyme complex (this sequence has the duration τ_1); the product is released from the state shown as the white circle; the blue circle indicates a sequence of recovery states (of duration τ_2) leading to the return of the enzyme to its initial state.

notations correspond to those used in Fig. 1. The segments of black lines indicate the intervals of time during which a given enzyme has been found in its initial state, waiting for the substrate binding event. The elongated red-white-blue graphic elements show the molecular catalytic cycles: the red color indicates the molecular states of the substrate-enzyme complex, the white color shows the state when the product molecule is being released, and the blue color shows motion through the recovery states, ending with the return of the molecule to its initial state. The bottom part of Fig. 2a shows the total number of the product molecules in the compartment as function of time, which corresponds to the above-presented molecular enzymic dynamics. The time is measured in units of the duration of a single molecular cycle τ_0.

Fig. 2b displays the histogram of the respective distribution of the entire enzymic population over different cycle phases, i.e. the number of enzyme molecules which are found at a fixed time moment in the molecular states corresponding to various values of the phase variable ϕ. The same color scheme as in Fig. 2a is used here to characterize different enzymic cycle stages.

We see that, as can be expected in this case, the cycles of individual enzymes are not correlated. Since allosteric regulation is not effective, binding of the substrate molecules occurs mainly by spontaneous, non-activated events. The waiting times are relatively long and therefore a significant fraction ($N_0 > 150$) of the enzyme molecules is found in the waiting state, as revealed by the high peak at $\phi = 0$ in Fig. 2b. The active molecules are almost uniformly distributed

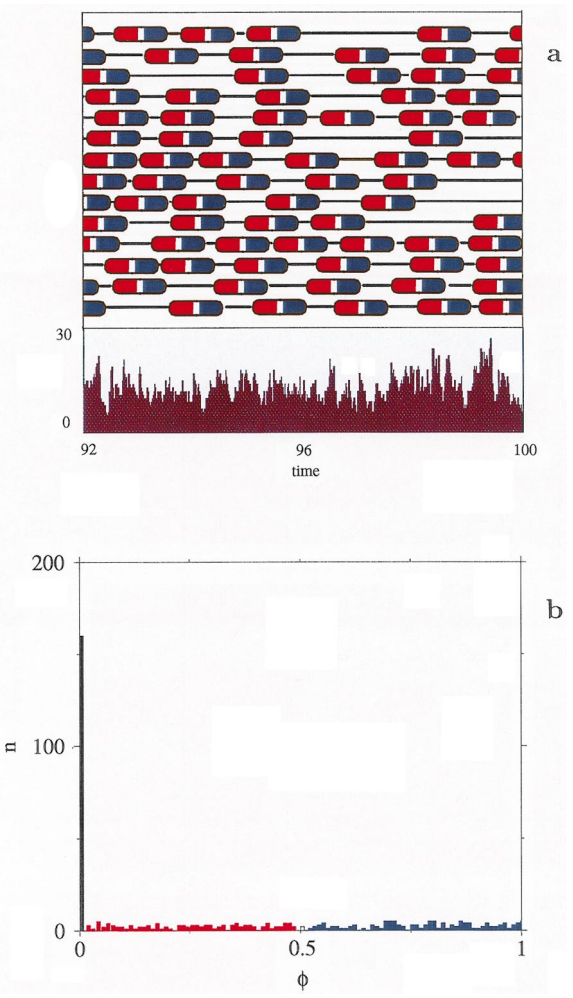

Fig. 2. Asynchronous molecular dynamics of the allosteric enzymatic reaction (Eq. (8)) for a population of $N = 400$ enzymes with the parameters $\gamma/\tau_0 = 20$, $\alpha_0/\tau_0 = 1$, and $\tau_1/\tau_0 = 0.5$ at low intensity of allosteric activation $\alpha_1/\tau_0 = 0.05$. Time is measured in units of the duration τ_0 of single molecular cycle. The upper part (a) displays individual molecular dynamics of 14 molecules which have been randomly selected from the whole interacting population; the bottom part (a) shows the respective number of product molecules in the compartment as function of time for this reaction (time is measured in units of the duration τ_0 of single molecular cycle). The histogram (b) displays the typical distribution of enzyme molecules over different cycle phases at a fixed time; the black peak at $\phi = 0$ shows the number of enzyme molecules in the free initial state, waiting to bind a substrate.

over various cycle phases. The number of product molecules in the compartment shows only random statistical variations around a certain mean level (Fig. 2a, bottom); the intensity of these fluctuations agrees with the predictions of a simple Poissonian statistics for uncorrelated reaction events.

The kinetic regime of this reaction is however completely changed (Fig. 3) when, while keeping fixed all other reaction properties, we increase the intensity of allosteric activation, specified by the parameter α_1. Looking at the upper part of Fig. 3a, one can see

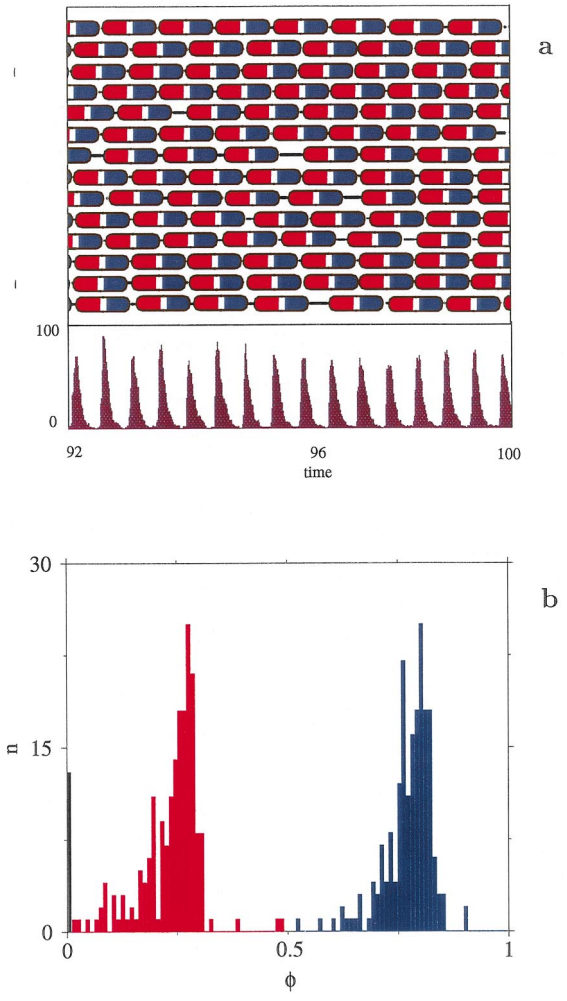

Fig. 3. Coherent two-group molecular dynamics of the enzymatic reaction (Eq. (8)) at a higher intensity of the allosteric activation $\alpha_1/\tau_0 = 0.5$. The same notations and parameter values as in Fig. 2. Time is measured in units of the duration τ_0 of single molecular cycle.

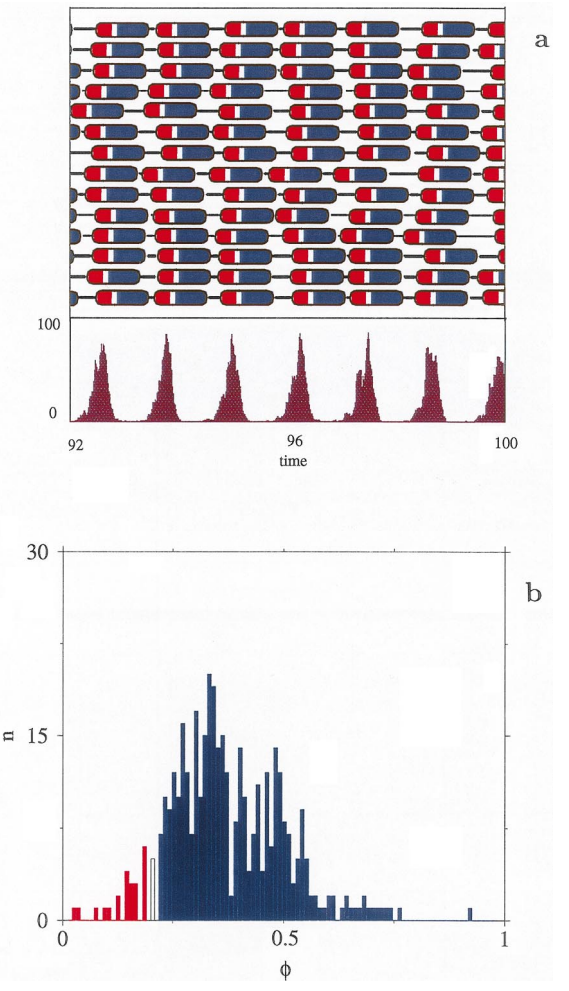

Fig. 4. Synchronous molecular dynamics of the entire enzymic population at $\tau_1/\tau_0 = 0.2$ and the same other parameters as in Fig. 3. Time is measured in units of the duration τ_0 of single molecular cycle.

that the enzymes are now divided into two synchronously operating molecular groups, whose catalytic cycles are shifted by approximately half a cycle period. These groups synchronously release the product molecules and therefore the dependence of the number of product molecules in the compartment on time (Fig. 3a, bottom) shows a sequence of sharp spikes. The period of this sequence is twice shorter than the molecular turnover time. Note that the life-time of product molecules is short and therefore all of them die before the next spike, caused by synchronous generation by a different enzymic group, appears. The two synchronous groups are clearly seen in the histo-

gram of the distribution over cycle phases in Fig. 3b. We see also in this histogram that the number of enzymes in the waiting state is now much smaller ($N_0 < 15$), which is a consequence of strong mutual allosteric activation.

Our analysis has revealed that the properties of the coherent reaction kinetics, realized at high intensities of allosteric regulation, significantly depend on the parameters of a single molecular cycle. By varying the relative time moment τ_1 inside a cycle, at which the product molecule is released, but keeping the total cycle duration $\tau_0 = \tau_1 + \tau_2$ constant, different kinetic regimes can be obtained. The behavior seen in Fig. 3 is realized when $\tau_1 = \tau_2 = 0.5\ \tau_0$ and therefore the product is released at the middle of a cycle.

As an example, Fig. 4 shows the kinetic regime which is found for the same reaction when the products are released soon after the cycle initiation, but their release is followed by a relatively long recovery time ($\tau_1 = 0.2\ \tau_0$, $\tau_2 = 0.8\ \tau_0$). We see that now the enzymes form a single coherent group (Fig. 4a, top) which yields spiking in the number of product molecules at a period close to the molecular turnover time (Fig. 4a, bottom). Remarkably, the life-time of product molecules is still much shorter than the cycle period. Indeed, almost all product molecules which were formed in a spike still die (Fig. 4a, bottom) before the next product generation arrives. The distribution over cycle phases is in this case relatively wide (Fig. 4b). When the precursor part of the group reaches the state where the product molecules are generated, the released product molecules activate the cycles of the rest of the group, terminating their waiting states.

Depending on the value of the ratio of τ_1 to τ_0, the regimes with different numbers of synchronous groups can be observed (see [5]). Recently we have developed the mean-field theory of the considered reaction and, by analyzing the stability of the asynchronous kinetic regime, have determined the bifurcation diagram which allows one to predict the number of coherent groups and the threshold of the transition to coherent molecular dynamics (to be published). This bifurcation diagram is shown in Fig. 5.

Thus, by analyzing a simple example of the product activated allosteric reaction (Eq. (8)) in a small compartment, when the conditions (Eq. (7)) of a molecular-network regime are satisfied, we have found that, for the higher intensities of allosteric regulation, this reaction undergoes a spontaneous transition to a coherent regime. In this regime, the entire enzymic population forms several synchronously operating groups which repeatedly activate the cycles of each other. Moreover, the analysis has revealed that the exact structuring of a population and the properties of the emerging coherent regime are strongly determined by the details of individual molecular cycles. By fluctuations, enzyme molecules can switch between the groups. Therefore, the numbers of molecules in each of the coherent groups are not exactly equal and statistically vary with time.

This analysis included a number of simplifications. For instance, we have neglected possible fluctuations during motion over the internal molecular reaction coordinates which would lead to a statistical dispersion in the durations of individual molecular cycles. Such fluctuations can easily be incorporated in the model. Our analysis shows that the coherent behavior may persist even when the dispersion of individual turnover times is so strong that it is comparable with its mean value.

We have already generalized our model to take into account a possibility that the regulatory product molecules spend a longer time, bound to the enzymes, and are thus removed from the solution. Moreover, variations in the substrate concentration in the compartment have also been taken into account. As will be shown in a separate publication, these effects do not eliminate the transition to coherent molecular dynamics, but only change its quantitative properties. Moreover, spiking in small compartments has also been found by us in the case of allosteric inhibition (to be published).

4. Coherence in coupled dynamical networks

In the previous section, we have shown how a network formed by an allosterically activated reaction can operate in the coherent mode. This network was very simple: the product of any enzyme could trigger the catalytic cycle of any other enzyme molecule. The biochemical networks of a living cell are much more complicated. Each of them can include various kinds of enzymes and regulatory molecules. Moreover, the same regulatory molecules can play an activatory role

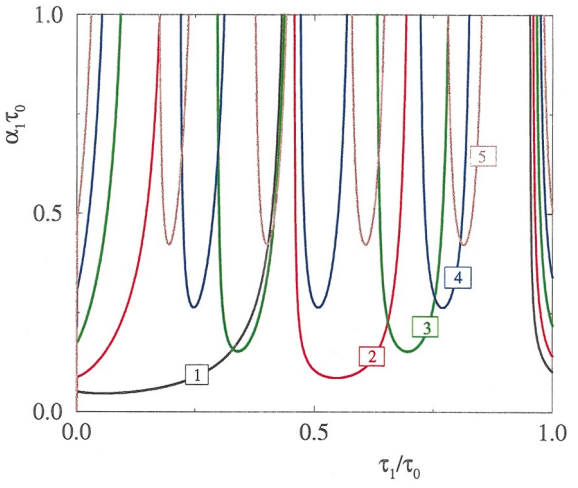

Fig. 5. The bifurcation diagram for the dynamical instability leading to spiking in the reaction (Eq. (8)) for $N = 1000$ enzymes and the reaction parameters $\alpha_0/\tau_0 = 1$ and $\gamma/\tau_0 = 20$. Spiking with different numbers of coherent molecular groups develops when the boundaries shown in the figure are crossed while moving up from the region of low intensity of the allosteric activation α_1/τ_0 at a constant ratio τ_1/τ_0. The boundaries correspond to the onset of spiking with two groups (red curves), three groups (green curves), four groups (blue curves), five groups (brown curves). The black curves indicate the onset of synchronous spiking of the whole population.

for some of the enzymes and inhibit the activity of the others. Different molecular networks can be cross-coupled, forming a larger supernetwork. Therefore, there is a question whether synchronization and coherent collective dynamics are also possible in the complex networks or in their ensembles.

We approach this question below by considering the collective dynamics in the ensemble of cross-coupled idealized neural networks. A formal neuron [19] is an automaton that can change its activity in response to signals arriving from other neurons. A network consists of a set of such elements linked through activatory or inhibitory connections. The dynamics of a network with arbitrary asymmetric connections is typically characterized by an irregular sequence of complex activity patterns. Hence, we can see that the model of a neuron network has some common properties with the molecular networks which are investigated in this paper. If synchronization is possible in an ensemble formed by such networks, it appears probable when cross-coupled molecular networks are considered.

We have analyzed by means of numerical simulations the collective behavior in ensembles consisting of a large number of identical neural networks, where the connection weights between neurons and their signs have been chosen at random.

The collective dynamics of the ensemble is described by the following algorithm. Each of N identical networks in the ensemble consists of K neurons. At the next discrete time moment $t + 1$, the activity x_k^i of a neuron $k = 1\ldots K$ belonging to a network $i = 1\ldots N$ is

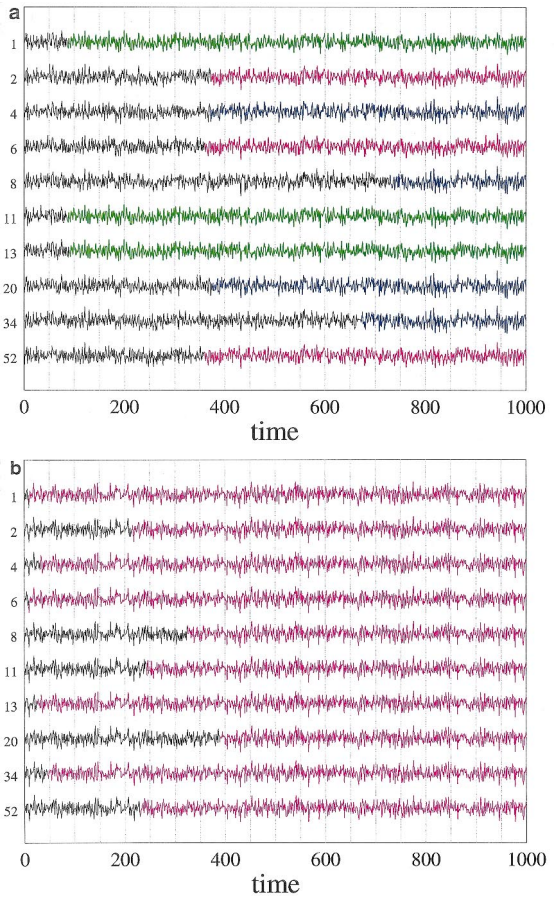

Fig. 6. Time-dependent integral activity $u_i(t)$ of 10 selected networks in an ensemble of 100 identical networks each consisting of 50 neurons for different intensities of global coupling, corresponding to (a) dynamical clustering ($\epsilon = 0.35$) and (b) complete synchronization ($\epsilon = 0.5$). Synchronous signals are indicated by the same colors. Random initial conditions, random choice of synaptic connection weights inside a network.

$$x_k^i(t+1) = (1-\epsilon)\theta(h_k^i) + \epsilon\theta\left(\sum_{j=1}^{N} h_k^j\right) \quad (13)$$

where

$$h_k^i = \sum_{l=1}^{K} J_{kl} x_l^i(t)$$

is the signal arriving to this neuron from all other elements of the same network, J_{kl} are the connection weights (the same for all networks), and $\theta(z)$ is a sigmoidal function, such as $\theta(z) = 0$ for $z < 0$ and $\theta(z) = 1$ for $z > 0$.

The two terms in the right side of Eq. (13) have a clear interpretation. The first of them represents the individual response of a neuron to the total signal received from all other elements in its own network. The second term depends on the global signal obtained by summation of individual signals received by neurons occupying the same positions in all networks of the ensemble. The parameter ϵ specifies the strength of global coupling. When global coupling is absent ($\epsilon = 0$), the networks forming the ensemble are independent. On the other hand, at $\epsilon = 1$ the first term vanishes and the states of respective neurons in all networks must be identical since they are completely determined by the same global signal. For $0 < \epsilon < 1$, the ensemble dynamics is governed by an interplay between local coupling inside the networks and global coupling between them.

We have found that this model exhibits, under increasing the global coupling intensity, a spontaneous transition to a coherent collective behavior. Such a transition is characterized by formation of the coherent network clusters followed by complete synchronization of all networks in the ensemble. It takes place already at low intensities of global coupling and is observed under an arbitrary choice of the connection weights in elementary networks and for random initial conditions. In our numerical simulations we have usually taken 100 networks, each consisting of 50 neurons.

Fig. 6 shows the typical results of these simulations. The integral time-dependent activity

$$u_i(t) = \sum_{k=1}^{K} x_k^i(t)$$

of 10 selected networks in the ensemble is displayed here (this presentation is reminiscent of the EEG records where the signal coming from each electrode is an average of the neural activity in the respective brain area). The dynamical patterns of network activity are always very irregular. However, depending on the intensity of coupling between the networks, a varying degree of coherence can be discerned in these patterns.

At a low coupling intensity, the activity of different networks is not coherent. When, however, a larger intensity of coupling is chosen, the behaviour of the ensemble is qualitatively changed. As time goes on, the activity signals generated by some of the networks suddenly become exactly identical. Eventually, the whole ensemble breaks down into several coherent clusters, so that for all networks belonging to the same cluster the total activity is the same at all times (the identical signals generated by networks from the same cluster are shown with the same color in Fig. 6a). At higher intensities of global coupling (Fig. 6b), the activity of all networks in the ensemble becomes coherent. Quite remarkably, the coherent signals are still very complex and apparently chaotic.

The robustness of synchronization in coupled neural networks, which has been observed under an arbitrary choice of activatory and inhibitory connections between neurons and for the networks and ensembles of different sizes, may serve as an indication that the coherent dynamics is typical for the networks of various origins, including the biochemical molecular networks which are considered in this paper. Further statistical study of the synchronization phenomena in ensembles of coupled neural networks will be reported in a separate publication [20].

5. Conclusions and outlooks

Our analysis puts forward a task of experimental observation of coherent molecular dynamics in allosterically regulated enzymatic reactions. Of course, turning from simple idealized models to real biochemistry brings new questions and problems. Most of them are related to the fact that until now the molecular dynamics of a single catalytic cycle of an enzyme molecule has not been well studied. It is not clear what are the statistical variations of turnover times of different enzymes and which physical prop-

erties may control these variations. The recovery time needed by an enzyme molecule to return to the initial state after releasing a product has never been experimentally investigated, though it plays an important role in determining the mode of coherent dynamics. Moreover, the molecular details of the allosteric regulation are also uncertain. The additional difficulties are caused by the condition that experiments should be performed for reactions in small micrometer-size compartments and would involve only hundreds or thousands of enzyme molecules. Nonetheless, the rapid progress of experimental methods may make such experiments feasible in the near future.

An experimental observation of coherent molecular dynamics would not only yield a proof that such processes are possible in real systems, including the living cells. They would also provide a new tool for investigating the details of individual molecular cycles by taking a population of enzyme molecules and synchronizing their individual dynamics.

In Section 1 we have compared a living cell with a large industrial factory where thousands of interconnected assembly lines are running in parallel to make a great variety of products. Some of these assembly lines may operate in the synchronous mode, while the operation of others can be asynchronous.

The employment of synchronous network organization has several important advantages. It can lead to a significant increase in the production efficiency of a reaction, as compared with its output in the usual non-correlated kinetic regime. Moreover, the coherent molecular networks are much more flexible in the functional sense. We have seen in Section 3, where a single product-activated enzymatic reaction was considered, that the same reaction can exhibit different forms of dynamic organization depending on the parameters of individual molecular cycles. The entire enzymic population breaks into several synchronously operating groups which activate one another.

These groups build, on the basis of the same underlying molecular network, various functional networks where each node is formed by a group of coherently operating elements and the links between the nodes indicate interactions between different functional groups. This phenomenon of emergent functional self-organization of a molecular network would become even more complex and significant when the networks consisting of several kinds of enzymes and comprising both activatory and inhibitory interactions are considered.

The networks operating in a coherent dynamical mode generate periodic frequent spikes of product molecules. The presence of such frequent generators inside a cell may be important because they can be used to externally synchronize other reactions, if the product molecules of a coherently operating network are used as substrate or regulatory molecules for these other reactions. Switching of the generation frequency can then control a transition to a different organization mode of the larger biochemical system.

Furthermore, not only the frequency but also the phase difference are important for controlling the coherent molecular dynamics. Indeed, when a short intensive spike of regulatory molecules arrive, it can execute its regulatory action only if the respective enzyme molecules are found at this time in that part of their molecular cycles where they are responsive to a regulation. For the complicated branched reaction schemes it might mean that the same reaction would yield different kinds of final products depending on the fine phase tuning, if this reaction is operating in the non-classical regime of a molecular network. These arguments show that self-organizing molecular networks can play an important role in the molecular biology of a cell.

Acknowledgements

The authors acknowledge financial support from ‘Peter und Traudl Engelhorn Stiftung zur Förderung der Biotechnologie und Gentechnik’ (Germany), from Alexander von Humboldt-Stiftung (Germany), and from Fundacion Antorchas (Argentina). We are grateful to J. Holzwarth and R. Rigler for the discussions concerning experimental aspects of the problem.

References

[1] B. Hess, A.S. Mikhailov, Science 264 (1994) 223.
[2] B. Hess, A.S. Mikhailov, Ber. Bunsenges. Phys. Chem. 98 (1994) 1198.
[3] B. Hess, A.S. Mikhailov, J. Theor. Biol. 176 (1995) 181.
[4] B. Hess, A.S. Mikhailov, Biophys. Chem. 58 (1996) 365.
[5] A.S. Mikhailov, B. Hess, J. Phys. Chem. 100 (1996) 19059.

[6] R. Kapral, K. Showalter (Eds.), Chemical Waves and Patterns, Kluwer, Dordrecht, 1995.
[7] A. Goldbeter, Biochemical Oscillations and Cellular Rhythms, Cambridge University Press, Cambridge, 1996.
[8] B. Hess, Quart. Rev. Biophys. 30 (2) (1997) 121.
[9] H.C. Berg, Random Walks in Biology (Princeton University Press, Princeton, NJ, 1983.
[10] H. Gutfreund, Kinetics for the Life Sciences: Receptors, Transmitters, and Catalysis, Cambridge University Press, Cambridge, 1995.
[11] M. von Smoluchowski, Phys. Z. 17 (1916) 557.
[12] M. Eigen, Z. Phys. Chem. (München) 1 (1954) 176.
[13] G. Adam, M. Delbruck, Reduction of dimensionality in biological diffusion processes, In A. Rich and N. Davidson (Eds.), Structural Chemistry and Molecular Biology, Freeman, San Francisco, CA, 1968, 198 pp.
[14] J.B. Wittenberg, B.A. Wittenberg, Annu. Rev. Biophys. Chem. 19 (1990) 217.
[15] L. Stryer, Biochemistry, 3rd edn., Freeman, New York, 1988.
[16] L.A. Blumenfeld, A.N. Tikhonov, (Eds.), Biophysical Thermodynamics of Intracellular Processes. Molecular Machines of the Living Cell, Springer, Berlin, 1994.
[17] N. Wiener, A. Rosenblueth, Arch. Inst. Cardiol. Mex. 16 (1946) 205.
[18] A.S. Mikhailov, Foundations of Synergetics. I. Distributed Active Systems, Springer, Berlin, 1990, 2nd rev. edn., 1996.
[19] W.C. McCulloch, W. Pitts, Bull. Math. Biophys. 5 (1943) 115.
[20] D. Zanette, A.S. Mikhailov, Phys. Rev. E (1998) in press.